Research Article

Advances in Mechanical Engineering

Advances in Mechanical Engineering
2016, Vol. 8(11) 1–8

DOI: 10.1177/1687814016677659
aime.sagepub.com
SAGE

Molecular dynamics studies on the overall compressive modulus of nylon 6/montmorillonite nanocomposites

Wen Xu[1], Xiaolei Wu[2] and Weifu Sun[3,4]

Abstract

Molecular dynamics simulations together with micromechanics method have been proven an effective approach to assess the elastic moduli of either partially or fully exfoliated (i.e. single-layer) effective clay (montmorillonite) cluster. In this work, similar approach was adopted to estimate the overall compressive modulus of nylon 6/montmorillonite nanocomposites. In detail, the compressive modulus of single-layer effective clay cluster along either lateral or longitudinal directions was first determined by performing molecular dynamics simulations, and then, the compressive modulus of partially exfoliated two-layer or three-layer effective clay clusters along the longitudinal direction was measured in a similar way. Finally, the overall compressive moduli of clay-incorporated polymer nanocomposites with either randomly dispersed or well-aligned effective clay clusters at different volume fractions of clay were evaluated according to the individual compressive modulus using the well-established rule of mixture.

Keywords

Clay, montmorillonite, nanocomposites, molecular dynamics, compressive modulus

Date received: 13 February 2016; accepted: 13 October 2016

Academic Editor: Filippo Berto

Introduction

Clay-based polymer nanocomposites have exhibited many advanced properties such as significantly reinforced mechanical properties (e.g. elastic moduli),[1–6] greatly improved thermal stability,[7,8] excellent gas barrier properties[9,10] and dielectric properties.[11,12] Among these fantastic properties of polymer/clay nanocomposites, enhanced mechanical properties have attracted a lot of interest and attention. This is because the incorporation of nanoclay into polymer matrix at a small volume fraction could have an obvious reinforcing effect on the enhancement in mechanical properties. The origin of this reinforcement effect can be largely attributed to the large ratio of surface area to volume and excellent cation exchange ability of montmorillonite, thus giving rise to strong interactions between polymer matrix and clays.[13,14] Among the mechanical properties, tensile modulus and compressive modulus are the two most important mechanical properties of polymer nanocomposites. Generally, these two moduli should have similar values, but they can be expected to have slightly different values probably due to the different load transfer behaviours.[5,15] Much effort, either experimental or theoretical, has been devoted to

[1]College of Materials and Mineral Resources, Xi'an University of Architecture and Technology, Xi'an, China
[2]School of Metallurgical Engineering, Xi'an University of Architecture and Technology, Xi'an, China
[3]School of Aerospace, Mechanical and Mechatronic Engineering, The University of Sydney, Sydney, NSW, Australia
[4]School of Chemical Engineering, University of Birmingham, Birmingham, UK

Corresponding author:
Weifu Sun, School of Aerospace, Mechanical and Mechatronic Engineering, The University of Sydney, Building J07, Sydney, NSW 2006, Australia.
Email: weifu.sun518@gmail.com; w.sun.1@bham.ac.uk

determine the elastic moduli of clay-based polymer nanocomposites over last decades. Numerically speaking, attention so far has been paid to the finite element analysis together with micromechanics modelling of the mechanical properties of polymer–clay nanocomposites based on two- or three-dimensional model from the continuum or micro-level,[16–19] but most of them have put emphasis on the volume fraction of clay, level of exfoliation and flake orientation and so on. In contrast, the interfacial structure between clay and polymer, atomic structure of clays, surface effect, and so on are often ignored, and the intermolecular forces such as van der Walls (vdW) attraction and the short-range Born repulsion forces that are not so obviously important on the continuum or macro/micro-level play increasingly dominant role at the nanoscale.[20,21] Therefore, much work is needed to be performed to take into account the interfacial microstructure and intermolecular forces from the atomic/molecular scale. What is more, most of the previous works are associated with tensile modulus, while the prediction of compressive modulus is often neglected,[22] and there remains a great need for better understanding the compression behaviours of materials and the underlying mechanisms in order to strengthen one's ability to predict the mechanical properties and boost the development of polymer–clay nanocomposites. In practice, a spectrum of advanced experimental approaches has been developed to prepare polymer/clay nanocomposites to improve the dispersion of clay within the polymer matrix, such as chemical modifications of polymer matrix,[23] pretreatment of clay[24] and master batch.[25] However, its reproducibility is affected by many factors and requires rigorous control of experimental conditions. Thus, molecular dynamics (MD) simulation, as an alternative tool, has a valuable role to play in providing almost exact results from atomic/molecular level.[20,26]

Experimentally, Schadler et al.[27] characterised both compressive modulus and tensile modulus of carbon nanotube/epoxy composites and found that there is a better load transferring behaviour when the composites are subjected to compression than being subjected to tension. They attributed such phenomenon to the rationale that when the composites are under compressive stress, easier load transfer can pass through the inner layers of multiwalled nanotubes (MWNTs) due to the easy buckling and bent sections of the nanotubes. Theoretically, Brune and Bicerano[5] developed a model to compare the tensile and compressive moduli of nanocomposites, and they found that a reduction in compressive modulus occurred relative to the tensile modulus. However, it is still theoretically challenging to predict the compressive modulus of polymer nanocomposites, and an effective approach is still to be well developed.

In our previous work, Young's moduli of nylon 6/clay nanocomposites have been predicted using the MD simulation along with conventional micromechanics method, and the developed approach has been well validated by comparing with experimental data.[22] In this work, similar approach will be adopted to calculate the compressive moduli of individual clay, effective nylon 6/clay clusters, and then, the overall compressive of polymer nanocomposites will be evaluated using the similar approach to Young's modulus. In detail, the compressive moduli of either fully exfoliated or partially exfoliated two-layer and three-layer effective clay clusters are first calculated using the MD simulations. Then, the overall compressive moduli of polymer–clay nanocomposites under various conditions (e.g. well-aligned effective clay clusters, randomly dispersed effective clay clusters within the polymer matrix) will be predicted using the micromechanics method of rule of mixtures. Finally, a comparison will be made between the compressive moduli and tensile moduli of nylon 6/montmorillonite (MMT) nanocomposites.

Simulation method

Model construction

The three effective clay clusters including single-, two- and three-layered clay clusters are built in the same way as done before.[22] The three structures are shown in Figure 1. Note that the basal spacing of octadecyltrimethyl ammonium–modified montmorillonite (ODTMA-MMT) is 22.3 Å.[22]

Simulation conditions

The setting parameters including force field, the algorithm and the controlling methods of temperature and

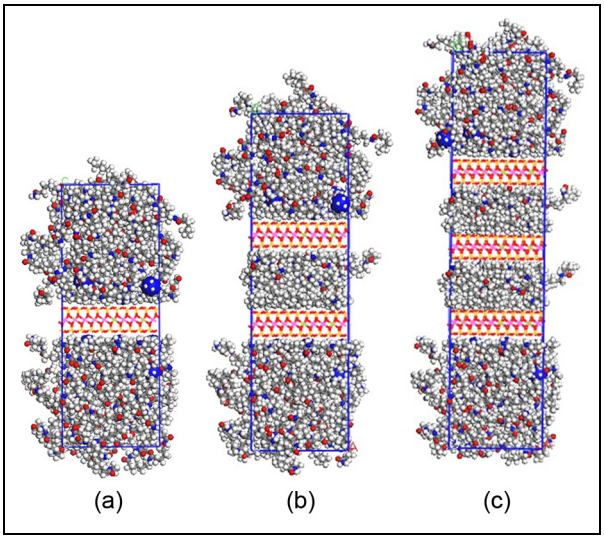

Figure 1. The three effective clay clusters: (a) fully exfoliated single-layer effective clay clusters, (b) partially exfoliated two-layer effective clay clusters and (c) partially exfoliated three-layer effective clay clusters.

pressure are adopted in a similar way as reported before.[22] In this work, three effective clay clusters were subjected to compressive stress along the longitudinal direction (Z-axis) in order to determine their compressive moduli, and five gradually increased compressive stresses were applied to the three effective clay clusters. The MD simulations were performed using isothermal–isobaric NPT ensemble (i.e. constant atom number, constant pressure and constant temperature) and velocity Verlet integration algorithm with a time step of 1 fs (1.0×10^{-15} s). After the first external compressive stress was applied to the structure, NPT simulation was carried out for 100 ps, and data were collected from the last 50 ps to analyse the compressive modulus using discover analysis module. The final structure was then exported and fully relaxed using NVT ensemble (i.e. constant atoms, constant volume and constant temperature), followed by being subjected to a higher external compressive stress to obtain the corresponding compressive modulus. Finally, the as-obtained five compressive moduli of effective clay clusters were averaged. Apart from the longitudinal Z-axis direction, compressive moduli of fully exfoliated single-layer effective clay cluster along the lateral directions (e.g. X- or Y-axis) were also determined using the same calculation method, which will be used to predict the overall compressive modulus of nanocomposites.

Overall compressive moduli of nylon 6/MMT nanocomposites with randomly dispersed or well-aligned effective clay clusters

The compressive moduli of randomly dispersed effective clay clusters and the overall compressive moduli of nylon 6/MMT nanocomposites can be obtained based on statistical distributions and the rule of mixture, respectively. The detailed calculation process and governing equations can be found in the previously published work.[22]

Results and discussion

Compressive modulus of effective clay clusters

MD simulations were carried out to determine the compressive moduli of fully exfoliated effective clay cluster along both the lateral direction (E_{11}) and longitudinal direction (E_{33}). Likewise, those of partially exfoliated (two or three layer) effective clay clusters along the longitudinal direction (E_{33}) were also obtained in a similar way. The results are listed in Tables 1–3, respectively. Continuous compressive stresses were applied to these three structures. That is, for single-layer clay cluster, compressive stress of 0.6–1.0 MPa along the lateral direction and 6–10 MPa along the longitudinal direction was applied, whereas compressive stress ranging from 5 to 9 MPa was employed for partially exfoliated effective clay clusters along the longitudinal direction. However, as observed from Tables 1–3, the results obtained are not sensitively dependent on the applied stresses, at least in the considered range.

The calculated compressive moduli of these three structures along longitudinal direction E_{33} are 35.6 ± 1.25, 52.4 ± 2.94 and 61.3 ± 4.16 GPa, respectively. In our previous work, the obtained Young's moduli of these three structures along the longitudinal direction E_{33} are 36.8 ± 3.22, 51.7 ± 2.26 and 60 ± 0.98 GPa, respectively. It can be observed that

Table 1. The calculated compressive moduli (E_{11}, GPa) of single-layer effective clay cluster along the lateral direction.

Applied stress (MPa)	0.6	0.7	0.8	0.9	1	Average
E_{11}	33.8	37.5	38.0	38.5	34.4	36.4 ± 1.25

Table 2. The calculated compressive moduli (E_{33}, GPa) of single-layer effective clay cluster along the longitudinal direction.

Applied stress (MPa)	6	7	8	9	10	Average
E_{33}	35.0	34.0	37.4	35.9	35.8	35.6

Table 3. The calculated compressive moduli (E_{33}, GPa) of partially exfoliated two- and three-layer effective clay clusters along longitudinal direction.

Applied stress (MPa)	5	6	7	8	9	Average
E_{33} (two layer)	50.2	50.6	54.9	56.2	50.0	52.4 ± 2.94
E_{33} (three layer)	58.5	64.8	64.2	55.4	63.7	61.3 ± 4.16

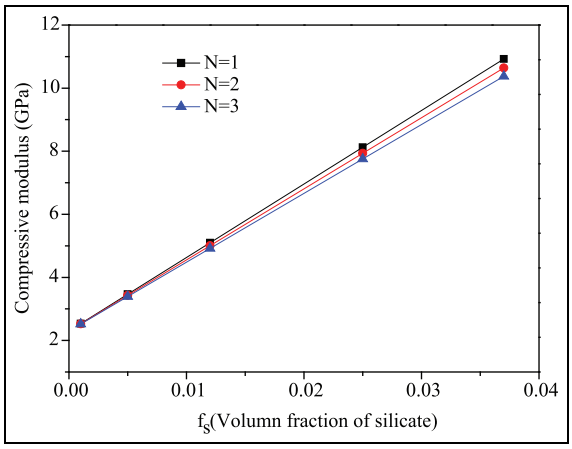

Figure 2. Overall compressive moduli of nylon 6/MMT nanocomposites incorporating clay clusters containing different numbers *N* of clay platelets in a typical stack (with d_{001} = 2.23 nm).

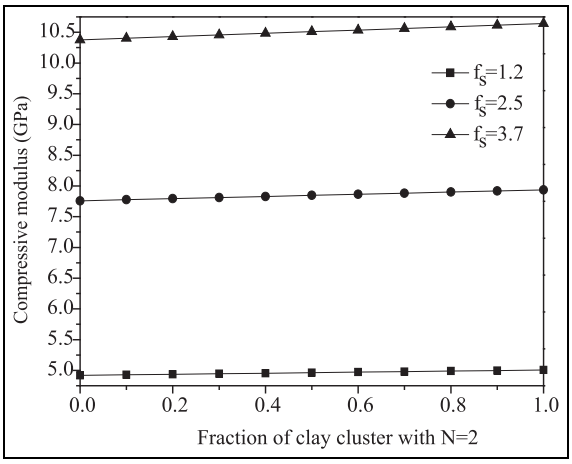

Figure 3. Compressive moduli of nylon 6/MMT nanocomposites at different fractions of two-layer effective clay clusters while the total volume fraction of silicate clay f_s is 1.2, 2.5 and 3.7 vol%.

these two mechanical properties (i.e. compress moduli and Young's moduli) of these effective clay clusters have almost the same values, but the compressive moduli are slightly larger than Young's moduli to a larger degree. Similar phenomena have been widely observed in experimental and computational measurements,[28] which is often referred to as 'hardening effect'. The rationale for such difference possibly lies in the high pressure inside the particle during the compressing process.[29]

Overall compressive moduli of nylon 6/MMT nanocomposites with well-aligned unitary effective clay clusters

The overall compressive moduli of nylon 6/MMT nanocomposites can be calculated in virtue of the individual compressive moduli of either effective clay cluster or polymer matrix. The volume fraction of clay f_c is here supposed to be 0.1, 0.5, 1.2, 2.5 and 3.7 vol%. And, N (= 1, 2, 3) represents the average number of silicate layers in the effective clay clusters, corresponding to fully exfoliated single-layer (N = 1), partially exfoliated two-layer (N = 2) and three-layer effective clay clusters (N = 3), respectively. As shown in Figure 2, there is no much difference in compressive moduli for fully and partially exfoliated morphologies. But it is still clear that fully exfoliated morphology exhibits the largest compressive moduli among the three effective structures. Similar phenomena have also been observed elsewhere,[5] indicating that incomplete exfoliation has an obvious adverse effect on the reinforcement of polymer nanocomposites. Because the polymer matrix is sandwiched between clay layers, this will increase the spacing distance of the stacks and decrease the effective aspect ratio of clays. Therefore, a lower effective modulus compared with the fully exfoliated clay clusters will be generated.

Overall compressive moduli of nylon 6/MMT nanocomposites incorporating with well-aligned binary effective clay clusters

As confirmed from transmission electronic microscopy (TEM) by Anoukou et al.,[4] when the loading of clay is high, for example, 1.2, 2.5 and 3.7 vol%, it is mainly partially exfoliated clay clusters that are distributed within polymer matrix. Therefore, we assume that there exist only two- and three-layer effective clay clusters, and the evaluated results are shown in Figure 3. With the increase in volume fraction of two-layer effective clay clusters in nanocomposites, compressive moduli gradually increase. In particular, when the volume fraction of two-layer effective clay cluster equals 1 ($f_{s,\ two}$ = 1), that is, two-layer only, the nanocomposites reach a peak compressive modulus.

Overall compressive moduli of nylon 6/MMT nanocomposites with classical distribution of angle

In practice, the distribution of clay clusters within polymer matrix is treated to ideally follow the uniform distribution or adopts the Gaussian distribution. In such cases, the compressive moduli of polymer composites containing sole one-, two- or three-layer clay clusters are first calculated, and the results are listed in Table 4.

The overall compressive moduli of nanocomposites with classical distributions (either uniform distribution or Gaussian distribution) are shown in Figures 4 and 5,

Table 4. The calculated compressive moduli (GPa) of fully exfoliated (single-layer), two-layer and three-layer effective clay clusters when the angle θ follows uniform distribution and Gaussian distribution.

	Single-layer effective clay	Two-layer effective clay	Three-layer effective clay
Uniform distribution	45.8	56.5	62.2
Gaussian distribution	50.8	62.7	69.0

Table 5. Compressive moduli (GPa) of fully exfoliated single-layer effective clay cluster, partially exfoliated two-layer and three-layer effective clay clusters with different angles.

Clay layers	Angle (θ)				
	0°	30°	45°	60°	90°
$N = 1$	36.4	49.3	50.9	49.0	35.6
$N = 2$	36.4	57.7	62.8	63.6	52.4
$N = 3$	36.4	62.2	69.1	71.3	61.3

Table 6. Compressive moduli (GPa) of effective clay clusters with arbitrarily assigned distribution of angle θ.

Clay layers	Percentage of angles				
	0° (0%)	30° (25%)	45° (35%)	60° (20%)	90° (20%)
$N = 1$	0	12.3	17.8	9.8	7.1
$N = 2$	0	14.4	22.0	12.7	10.5
$N = 3$	0	15.6	24.2	14.3	12.3

respectively. It can be observed that Gaussian distribution predicts larger values of compressive moduli than uniform distribution does. This phenomenon is explainable in terms of the fact that the angle θ mainly locates between 40° and 60° in Gaussian distribution, and as observed from Table 5, the compressive moduli of effective clay clusters are relatively larger when the angle θ falls within 30°, 45° and 60°. It can be observed that given the identical angles, with the increase in the number of layers of clays, the compressive modulus gradually increases except the parallel condition ($\theta = 0°$); given the identical angle, the compressive modulus first increases gradually from 36.4 GPa, then reaches a peak at 45°, followed by a decrease. This might be understandable that at the optimum angle of $\theta = 45°$, sliding between clays can be mitigated to a minimum, and especially for the case of 90°, relative sliding or rolling between adjacent clays in the two-dimensional directions that readily leads to translation or rotation for the parallel orientation, can also be alleviated. Therefore, the interconnected network provides the highest compressive modulus. Besides, it observed from Figures 4 and 5 that fully exfoliated morphology ($N = 1$) predicts the largest value, whereas partially exfoliated morphologies ($N = 2$ and $N = 3$) give smaller and almost identical results. This conclusion has been well recognised that fully exfoliated morphology exhibits the largest mechanical properties.[4,5]

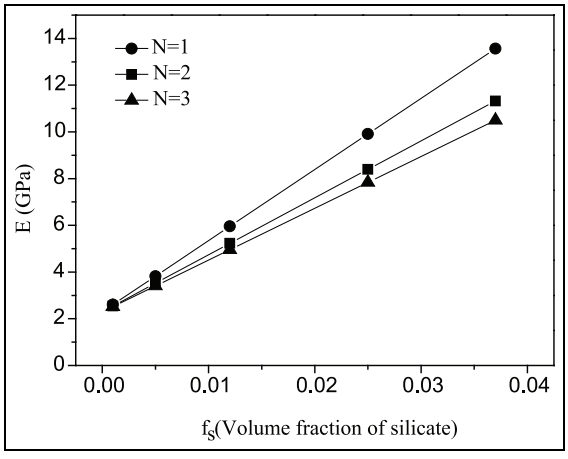

Figure 4. Overall compressive moduli of nylon 6/MMT nanocomposites for different numbers N of clay platelets in a typical stack (with $d_{001} = 2.23$ nm), in which the angle θ follows the uniform distribution.

Table 7. Randomly dispersed effective clay clusters when the angle θ distribution is determined based on experimental observation.

		0°	30°	45°	60°	90°
0.5%	$N = 1$	30%	30%	0%	20%	20%
1.2%	$N = 2$	80%	10%	0%	0%	10%
2.5%	$N = 3$	90%	0%	0%	0%	10%
3.7%	$N = 3$	90%	0%	0%	0%	10%

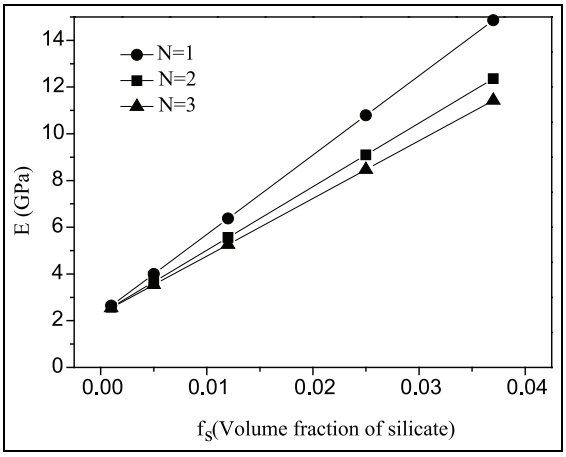

Figure 5. Overall compressive moduli of nylon 6/MMT nanocomposites for different numbers N of clay platelets in a typical stack (with $d_{001} = 2.23$ nm), in which the angle θ follows the Gaussian distribution.

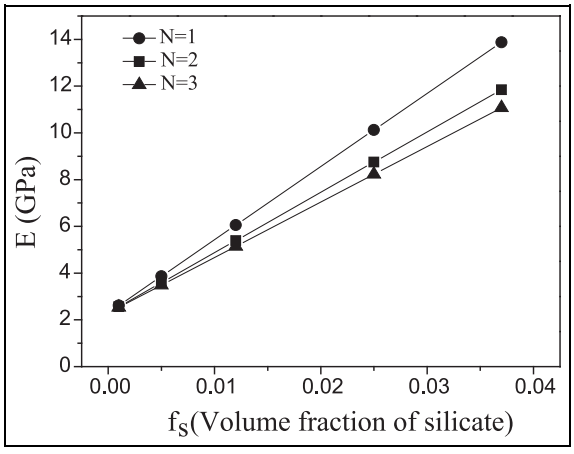

Figure 6. Overall compressive moduli of nylon 6/MMT nanocomposites for different numbers N of clay platelets in a typical stack (with $d_{001} = 2.23$ nm), in which the angle θ distribution is arbitrarily assigned, as shown in Table 6.

Overall compressive moduli of nylon 6/MMT nanocomposites when distribution of angle θ is arbitrarily assigned and based on experimental observation

In the previous work,[22] we have demonstrated that MD simulations of Young's moduli of nylon 6/MMT nanocomposites with random distribution of angle θ can satisfactorily reproduce the experimental data. Therefore, in this section, we will continue to use the same method to predict the overall compressive moduli of nanocomposites. The distribution of angle θ that is either arbitrarily assigned or determined based on experimental observation was applied, and the results are shown in Tables 6 and 7, respectively. Accordingly, the overall compressive moduli of nylon 6/MMT nanocomposites can be seen in Figures 6 and 7, respectively. As can be observed from Figure 6, the same and even ratios of angle θ were applied to both fully and partially exfoliated morphologies. However, Anoukou et al.[4] have reported that the clay platelets are dispersed in random angles when fully exfoliated clay platelet predominates in the nanocomposites; thus, our simulation data took the percentages of angles 0°, 30°, 45°, 60° and 90° as occupied by 30%, 30%, 0%, 20% and 20%, respectively. Moreover, the clay platelets are mainly located parallel to the applied force when partially exfoliated structures start to occur (i.e. the clay volume fractions are 2.5 and 3.7 vol%). Therefore, during the simulations, the percentages of angles 0° and 90° were given 90% and 10%, respectively, and our simulated results were shown in Figure 7.

Conclusion

Compressive modulus, as one of the important mechanical properties of polymer nanocomposites, was studied using MD simulations. In this work, the compressive moduli of polymer nanocomposites incorporated with clay clusters under either well-aligned or randomly dispersed circumstances were studied. The previously developed simulation approach together with traditional micromechanics method was further developed and extended to predict the overall compressive modulus of polymer nanocomposites. The simulation results show that the fully exfoliated clays deliver better compressive moduli of polymer nanocomposites than partly exfoliated clays; moreover, the nanocomposites give rise to the highest compressive modulus at the optimum angle of 45°, whatever be the types of exfoliated clays.

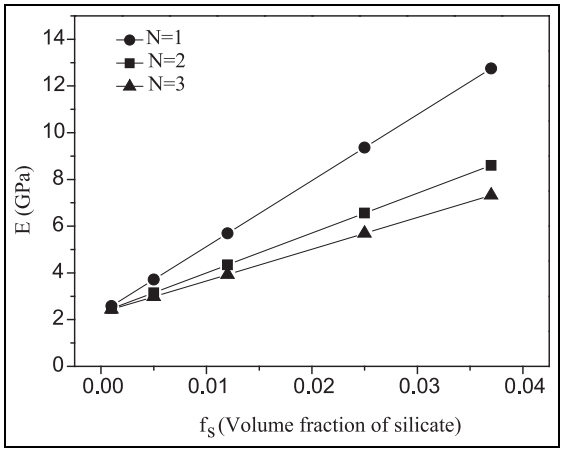

Figure 7. Overall compressive moduli of nylon 6/MMT nanocomposites for different numbers *N* of clay platelets in a typical stack (with d_{001} = 2.23 nm), in which the angle θ distribution is determined from experimental observation, as shown in Table 7.

It is believed that when the effective clay clusters are randomly located in the polymer matrix, our simulation data can reasonably predict the overall compressive moduli of nylon 6/MMT nanocomposites in practice.

Acknowledgements

The authors thank the support from the universities. W.X. and X.W. equally contributed to this work.

Declaration of conflicting interests

The author(s) declared no potential conflicts of interest with respect to the research, authorship, and/or publication of this article.

Funding

The author(s) disclosed receipt of the following financial support for the research, authorship, and/or publication of this article: This work is partly funded by the National Natural Science Foundation of China (grant no. 51504179), Foundation of Shaanxi Educational Committee (grant no. 15JK1437) and Talent Technology Fund of Xi'an University of Architecture and Technology (grant no. RC1402).

References

1. Ji XL, Jing JK, Jiang W, et al. Tensile modulus of polymer nanocomposites. *Polym Eng Sci* 2002; 42: 983–993.
2. Luo JJ and Daniel IM. Characterization and modeling of mechanical behavior of polymer/clay nanocomposites. *Compos Sci Technol* 2003; 63: 1607–1616.
3. Anoukou K, Zaïri F, Naït-Abdelaziz M, et al. On the overall elastic moduli of polymer–clay nanocomposite materials using a self-consistent approach. Part I: theory. *Compos Sci Technol* 2011; 71: 197–205.
4. Anoukou K, Zaïri F, Naït-Abdelaziz M, et al. On the overall elastic moduli of polymer–clay nanocomposite materials using a self-consistent approach. Part II: experimental verification. *Compos Sci Technol* 2011; 71: 206–215.
5. Brune DA and Bicerano J. Micromechanics of nanocomposites: comparison of tensile and compressive elastic moduli, and prediction of effects of incomplete exfoliation and imperfect alignment on modulus. *Polymer* 2002; 43: 369–387.
6. Mesbah A, Zaïri F, Naït-Abdelaziz M, et al. Micromechanics-based constitutive modeling of plastic yielding and damage mechanisms in polymer–clay nanocomposites: application to polyamide-6 and polypropylene-based nanocomposites. *Compos Sci Technol* 2014; 101: 71–78.
7. Dasari A, Lim SH, Yu ZZ, et al. Toughening, thermal stability, flame retardancy, and scratch–wear resistance of polymer–clay nanocomposites. *Aust J Chem* 2007; 60: 496–518.
8. Gilman JW. Flammability and thermal stability studies of polymer layered-silicate (clay) nanocomposites. *Appl Clay Sci* 1999; 15: 31–49.
9. Koh HC, Park JS, Jeong MA, et al. Preparation and gas permeation properties of biodegradable polymer/layered silicate nanocomposite membranes. *Desalination* 2008; 233: 201–209.
10. Mittal V. Gas permeation and mechanical properties of polypropylene nanocomposites with thermally-stable imidazolium modified clay. *Eur Polym J* 2007; 43: 3727–3736.
11. Phiriyawirut P, Magaraphan R and Ishida H. Preparation and characterization of polybenzoxazine-clay immiscible nanocomposite. *Mater Res Innov* 2001; 4: 187–196.
12. Vengatesan MR, Devaraju S, Dinakaran K, et al. Studies on thermal and dielectric properties of organo clay and octakis (dimethylsiloxypropylglycidylether) silsesquioxane filled polybenzoxazine hybrid nanocomposites. *Polym Composite* 2011; 32: 1701–1711.
13. Bharadwaj RK, Mehrabi AR, Hamilton C, et al. Structure–property relationships in cross-linked polyester–clay nanocomposites. *Polymer* 2002; 43: 3699–3705.
14. Giannelis E. A new strategy for synthesizing polymer-ceramic nanocomposites. *JOM: J Min Met Mat S* 1992; 44: 28–30.
15. Li CY and Chou TW. Multiscale modeling of compressive behavior of carbon nanotube/polymer composites. *Compos Sci Technol* 2006; 66: 2409–2414.
16. Fertig RS and Garnich MR. Influence of constituent properties and microstructural parameters on the tensile modulus of a polymer/clay nanocomposite. *Compos Sci Technol* 2004; 64: 2577–2588.
17. Saadatfar M, Khatibi AA and Mortazavi B. Effective parameters on the stress–strain curve of nylon 66/clay nanocomposite using FEM. *Strain* 2011; 47: e442–e446.
18. Hbaieb K, Wang QX, Chia YHJ, et al. Modelling stiffness of polymer/clay nanocomposites. *Polymer* 2007; 48: 901–909.
19. Saadatfar M and Soleimani M. Effective parameters on elastic modulus of polymer/clay nanocomposites. *Adv Mat Res* 2012; 403: 4416–4420.

20. Sun WF, Zeng QH and Yu AB. Calculation of noncontact forces between silica nanospheres. *Langmuir* 2013; 29: 2175–2184.
21. Sun WF, Li YC, Xu W, et al. Interactions between crystalline nanospheres: comparisons between molecular dynamics simulations and continuum models. *RSC Adv* 2014; 4: 34500–34509.
22. Xu W, Zeng QH and Yu AB. Prediction of the overall Young's moduli of clay-based polymer nanocomposites. *J Compos Mater* 2015; 49: 3459–3469.
23. Wan YJ, Gong LX, Tang LC, et al. Mechanical properties of epoxy composites filled with silane-functionalized graphene oxide. *Compos Part A: Appl S* 2014; 64: 79–89.
24. Chen WC, Lai SM, Yang CH, et al. Effect of clay types on the properties of Si lane compatibilzied metallocene polyethylene/clay nanocomposites. *Polym Polym Compos* 2015; 23: 451–460.
25. Li YC, Tang JG, Huang LJ, et al. Facile preparation, characterization and performance of noncovalently functionalized graphene/epoxy nanocomposites with poly(sodium 4-styrenesulfonate). *Compos Part A: Appl S* 2015; 68: 1–9.
26. Sun WF. Interaction forces between a spherical nanoparticle and a flat surface. *Phys Chem Chem Phys* 2014; 16: 5846–5854.
27. Schadler LS, Giannaris SC and Ajayan PM. Load transfer in carbon nanotube epoxy composites. *Appl Phys Lett* 1998; 73: 3842–3844.
28. Sun WF. The dynamic effect on mechanical contacts between nanoparticles. *Nanoscale* 2013; 5: 12658–12669.
29. Mook WM, Nowak JD, Perrey CR, et al. Compressive stress effects on nanoparticle modulus and fracture. *Phys Rev B* 2007; 75: 214112.